Analytical Methods

Accepted Manuscript

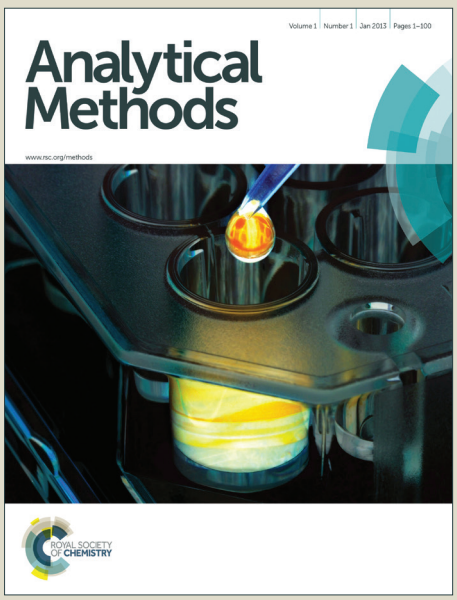

This is an *Accepted Manuscript*, which has been through the Royal Society of Chemistry peer review process and has been accepted for publication.

Accepted Manuscripts are published online shortly after acceptance, before technical editing, formatting and proof reading. Using this free service, authors can make their results available to the community, in citable form, before we publish the edited article. We will replace this *Accepted Manuscript* with the edited and formatted *Advance Article* as soon as it is available.

You can find more information about *Accepted Manuscripts* in the Information for Authors.

Please note that technical editing may introduce minor changes to the text and/or graphics, which may alter content. The journal's standard Terms & Conditions and the Ethical guidelines still apply. In no event shall the Royal Society of Chemistry be held responsible for any errors or omissions in this *Accepted Manuscript* or any consequences arising from the use of any information it contains.

ROYAL SOCIETY OF CHEMISTRY

www.rsc.org/methods

Cite this: DOI: 10.1039/c0xx00000x

www.rsc.org/xxxxxx

ARTICLE TYPE

An autonomous T-rich DNA machine based lateral flow biosensor for amplified visual detection of mercury ion

Jie Liu, ‡[a, c] Lingbo Chen, ‡ [b, a] Junhua Chen, [a] Chenchen Ge, [a] Zhiyuan Fang, [a] Lin Wang, [a] Xuerong Xing, [a, d]* and Lingwen Zeng[a]*

Received (in XXX, XXX) Xth XXXXXXXXX 20XX, Accepted Xth XXXXXXXXX 20XX
DOI: 10.1039/b000000x

An autonomous thymine rich DNA machine as an amplification unit was developed for the sensitive detection of mercury ion with high specificity. Combined with lateral flow biosensor, the amplified signal of Hg^{2+} can be read out by the naked eye with a detection limit of 5 nM.

Due to the toxic effect of mercury ion (Hg^{2+}) on human health and wildlife even at extremely low concentration, simple and cost-effective detection of Hg^{2+} contamination in food, drinking water and ecosystems gains a growing concern in the field of public health and environmental safety.[1] Presently, Hg^{2+} detection technologies, such as inductively coupled plasma-atomic emission spectrometry and atomic absorption spectroscopy, are becoming more sensitive with the development of sophisticated instrumentation and elaborate analytical techniques.[2] These modern instrumentation based approaches offer high sensitivity and accuracy for Hg^{2+} analysis, however, the requirement of sophisticated instrumentation and skilled personnel limits their point-of-use applications in resource limited settings.

To overcome the drawbacks and develop point-of-use approaches for simple and cost-effective Hg^{2+} analysis, some materials such as organic chromophores or fluorophores[3a], nanoparticles[3b], thin films[3c], proteins[3d], nucleic acids[3e, f] and polymers[3g] have been applied in the Hg2+ detection creatively. Among them, the application of nucleic acid is extremely attractive as they can form stable thymidine-Hg2+-thymidine (T-Hg2+-T) complexes that can offer high assay specificity for Hg2+ detection[4]; and most importantly, the advent of nucleic acid analysis techniques can promote the development of Hg^{2+} analysis tools for more extensive application. For example, nucleic acid analysis tools such as electrochemical ligands[5a], fluorophores[5b] and nanoparticles[3b] have been employed in Hg^{2+} analysis, which not only improved the sensitivity up to the level of pM, but also enriched the toolkit for Hg^{2+} analysis.

As a new nucleic acid tool in analytical science, DNA machine[6] has been successfully applied in the design of novel Hg^{2+} sensors. In these designs, DNA machines are viewed as molecular assemblies that perform consecutive mechanical operations, functioning as motors, rotors, switches or duplicator. During this detection process, the molecular machines are ignited by Hg^{2+}, leading to a structural change and then continuously yield a piece of DNA sequence (referred to as "waste product") that is later used as an amplified signal for Hg^{2+} in certain formats. For example, Willner *et al*. developed a T-rich DNA machine and achieved a highly sensitive Hg^{2+} analysis in colorimetric format.[3e] Afterwards, another DNA machine using silver nanoparticles as signal reporter was reported, which improved the sensitivity to 80 pM.[3f] The use of DNA machine enabled highly sensitive and specific Hg^{2+} detection, nevertheless, these methods face tough challenges in point-of-use applications. As noted above, the Willner *et al.* approach requires professional laboratory-type operations, such as precise transfer of solutions, which is unsuitable for people without scientific background; besides, it is less sensitive for instrument-free observation; and the latter method relies on an instrumental readout, and the silver nanoparticle has issues of kinetic instability, or aqueous incompatibility, which would affect the robustness of the Hg^{2+} assay. Therefore, it is highly desirable to develop a new Hg^{2+} analysis system that combines the advantages of DNA machine and advanced nucleic acid analysis techniques, to achieve sensitive, reliable, as well as simple, practical, cost-effective Hg^{2+} analysis.

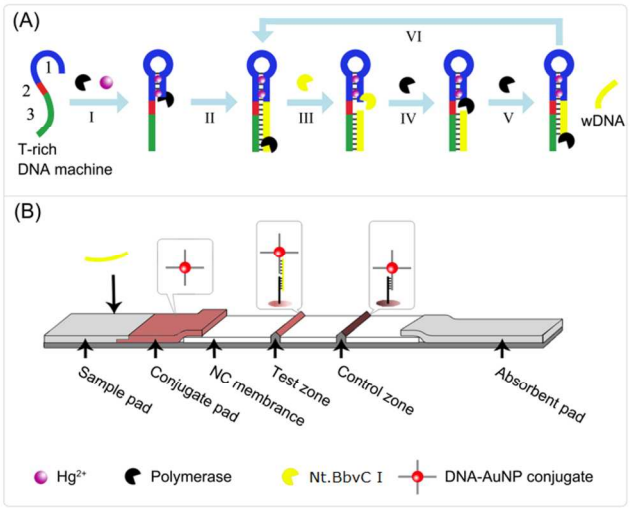

Scheme 1 (A) Schematic outline of the autonomous T-rich DNA machine for Hg^{2+} sensing. (B) Schematic illustration of the lateral flow biosensor for visual detection of Hg^{2+}.

Due to the simplicity, fast result reporting, cost-effectiveness, and user-friendliness, lateral flow biosensor (LFB) permits more applications for point-of-use in contrast to optical and

Analytical Methods Accepted Manuscript

electrochemical techniques.[7] In addition, compared with colorimetric methods, LFB possesses a better readability for the weak signal because of the strong contrast between the red signal line and the adjacent white membrane area. To expand DNA machine for point-of-use applications, it is of great interest to investigate the integration of DNA machine and LFB, which would possess not only the advantages of DNA machines but also the simplicity of LFB technique based platforms.

In this work, a Hg^{2+} ignited DNA machine was developed. Once triggered by Hg^{2+}, the machine would continuously yield waste product with the amount in response to the concentration of Hg^{2+}. Then the waste product was applied to a LFB, which converted the Hg^{2+} signal into a red line on the test zone of the biosensor, reaching a detection limit of 5 nM by the naked eye.

As shown in Scheme 1A, the Hg^{2+} ignited DNA machine has three regions (Table S1, ESI†). The blue domain ***1*** is the ignition system of the machine, including two T-rich regions linked by a DNA spacer. In the presence of Hg^{2+}, the T-rich regions hybridize to each other due to T-Hg^{2+}-T coordination chemistry. As a result, domain ***1*** switches to a hairpin conformation, forming a self-primed template structure[8]. Klenow fragment polymerase (KF) then binds to this structure to perform the replication of domain ***2*** and ***3***. Domain ***2*** contains the binding site of the nicking endonuclease Nt.BbvC Ⅰ and it is the heart of the machine where the machine's functions of replication and scission are operated. Domain ***3*** is the place where the waste product is generated and replaced. As shown in Scheme 1A, the DNA machine is ignited by Hg^{2+} to form a self-primed template (step Ⅰ). Subsequently, KF initiates the replication at the 3' end of the structure (step Ⅱ). Upon replication, Nt.BbvC Ⅰ recognizes its binding site and nicks the replicated strand (step Ⅲ). After nicking, KF moves to the 3' end of the nicked DNA and primes a new round of replication (step Ⅳ). During this replication, the complementary strand of domain ***3*** is displaced as the machine's waste product (wDNA) (step Ⅴ). Once the DNA machine is ignited by Hg^{2+}, the repeated operation of scission and replication continues to produce numerous wDNA (step Ⅵ), which is subsequently applied on a LFB for visual detection.

LFB consists of four components: a sample pad, a conjugate pad, a nitrocellulose membrane and an absorption pad (Scheme 1B). In this work, a 5'-thiol-modified 10-mer capture probe 1 (CP1), complementary with the 3' part of the wDNA, is conjugated with gold nanoparticles (AuNPs), and are dispensed on the conjugate pad. Another 10-mer 3'-biotin-modified capture probe (CP2), complementary with the 5' part of the wDNA, is immobilized on the test zone of nitrocellulose membrane via a streptavidin-biotin interaction[7]. Capture probe 3 (CP3), complementary with CP1, is immobilized on the control zone of the nitrocellulose membrane the same way as CP2 (see Table S1 in ESI† for the sequences of CP1, CP2, CP3). When the reaction mixture is applied to the sample pad of the LFB, the mixture passes the conjugate pad and rehydrates the AuNP-CP1 conjugates. The wDNAs in the mixture hybridize with CP1 to form the complexes of AuNP-CP1-wDNA and continue to migrate along the strip. The complexes are captured on the test zone by the second hybridization reaction between the wDNA and the immobilized CP2. Consequently, AuNPs accumulate on the test zone of the LFB to form a visible red line. In the absence of Hg^{2+}, no wDNA is generated, thus no red line appears on the test zone. The excess AuNP-CP1 conjugates continue to migrate and are captured on the control zone via the hybridization between CP1 and CP3, forming a second red line. In this case, a red line on the control zone shows that the LFB works properly. Qualitative analysis can be performed by observing the color change of the test zone, and quantitative detection can be realized by recording the optical density of the test zone with a portable strip reader.

As described above, the color intensity of test zone of the LFB corresponds with the concentration of Hg^{2+}. Fig. 1A shows the typical images of the LFB in response to various concentrations of Hg^{2+}. The intensity increased with the concentration of Hg^{2+}, and no red line was observed on the test zone in the absence of Hg^{2+}. Additionally, a linear correlation with the logarithm of the Hg^{2+} concentrations from 5 nM to 200 nM was obtained, allowing the color response for a wide range of concentrations of Hg^{2+} (Fig. 1B). A red line could be observed by the naked eye when as low as 5 nM of Hg^{2+} was present. So, 5 nM was used as the threshold for the visual Hg^{2+} analysis, which is much lower than the guideline value (30 nM) of the Hg^{2+} in drinking water set by the World Health Organization (WHO)[9].

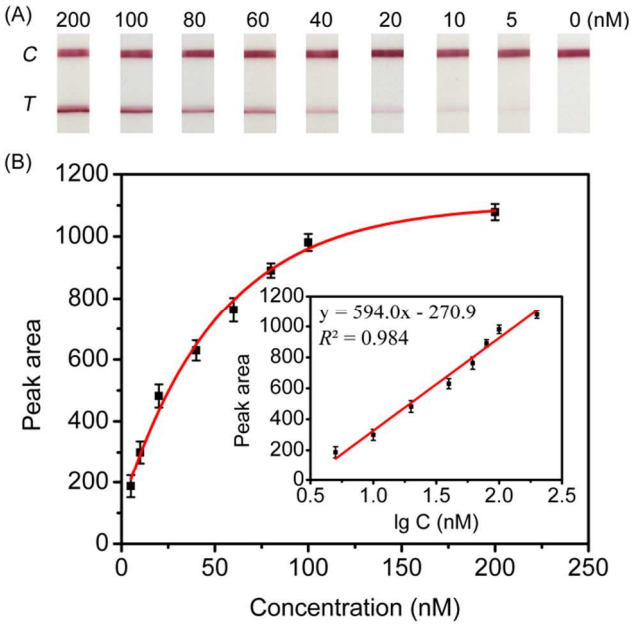

Fig. 1 (A) Photo images of LFBs after applying the product of T-rich DNA machine in the presence of various concentrations of Hg^{2+}. (B) Calibration curve of the assay with different concentrations of Hg^{2+}, values represent the intensity means ± s.d. of triplicate reactions.

Because cations would compete for the Hg^{2+} binding site on DNA machine to produce a false positive signal,[10] the specificity of this method was evaluated using 2 μM of the following cations, Mn^{2+}, Cd^{2+}, Mg^{2+}, Zn^{2+}, Fe^{3+}, Ba^{2+}, Ca^{2+}, Ni^{2+} and Co^{2+}. No red line was observed on the test zone (Fig. S1, ESI†), indicating that the designed DNA machine was selective to Hg^{2+}, which is due to the high binding constant of T-Hg^{2+}-T, 4.14×10^6 L mol^{-1}.[4] To further test the feasibility in practical use, the method was applied to analyze river water samples obtained from Pearl River (Guangzhou, China). The recovery experiments with spiked Hg^{2+} were carried out, and the satisfactory recovery rates were

Analytical Methods Accepted Manuscript

This journal is © The Royal Society of Chemistry [year]

obtained between 91.3% and 110.8% (Table S2, ESI†), which confirmed the feasibility of the method for Hg^{2+} analysis in river water samples that may include other potentially competing species. The above results demonstrated that the developed method can be used to screen Hg^{2+} contamination with high selectivity.

In this study, four important parameters were investigated for optimal analysis of Hg^{2+}.

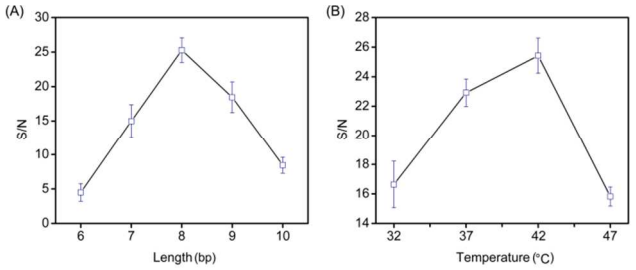

Fig. 2 Effect of the length of the primed-template structure (A) and temperature (B) on the S/N in the presence of Hg^{2+} of 80 nM, values represent the intensity means ± s.d. of triplicate reactions.

The length of the primed-template structure mentioned above affects the formation of hairpin conformation of domain ***1*** and KF activity for replication[8]. Thus, the primed-template structures of various length were designed (ESI†) and the optimum length was determined by comparing the ratio of signal to noise (S/N) in the presence of 80 nM Hg^{2+} at 37 °C. As shown in Fig. 2A, the S/N ratio rose with the length of the primed-template structure and dropped when the length is longer than 8 bp, hence the optimum length was 8 bp. It can be explained by that the structure shorter than 8 bp had low binding affinity to KF, resulting in low replication efficiency and low S/N ratio; whereas the structure longer than 8 bp induced the Hg^{2+}-independent formation of hairpin conformation of domain ***1***, which caused high background and low S/N ratio. Temperature is another important factor that affects the formation of the self-primed template, and the comparison of the S/N ratios at four temperatures shows that 42 °C was the optimum temperature (Fig. 2B), which could be attributed to the collective effect of the polymerase activity and the stability of the self-primed template.[8]

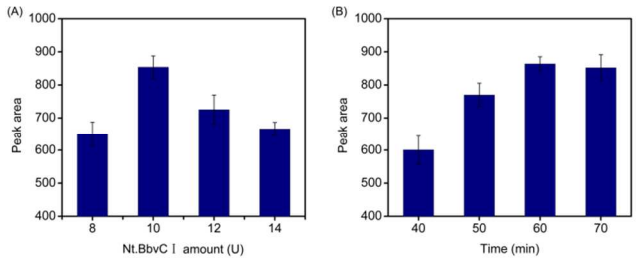

Fig. 3 Effect of the amount of Nt.BbvC Ⅰ (A) and incubation time (B) on the response of LFB in the presence of 80 nM Hg^{2+}, values represent the intensity means ± s.d. of triplicate reactions.

To function adequately with the DNA machine, Nt.BbvC Ⅰ must efficiently dissociate from the nicked site to allow the KF access in a coordinated way. One factor to affect the coordination would be the amount ratio of these two enzymes. Thus, the ratio was investigated by varying the quantity of Nt.BbvC Ⅰ while the amount of KF is fixed to 8U. As shown in Fig. 3A, the intensity of the test zone increased with the amount of Nt.BbvC Ⅰ raising to 10 U and decreased afterward, which suggested that 10U is the optimum amount to make two enzymes work together synergistically. This could be explained that the Nt.BbvC Ⅰ of high concentration dissociated slowly from the nicked site, leading to the slow access of KF, which reduced the efficiency of the DNA machine[11]. Under the above conditions, the intensity of the test zone increased with the incubation time from 40 to 60 min and then enhanced no further (Fig. 3B). Thus, 60 min was the optimum reaction time for the machine.

In conclusion, an amplified visual approach for Hg^{2+} analysis was developed. The integration of LFB with DNA machine enabled instrument-free readout with a detection limit of 5 nM, which is much lower than the maximum level (30 nM) of Hg^{2+} in drinking water permitted by the WHO. Complementary to instrumentation based methods, this instrument-free approach should offer a point-of-use solution for Hg^{2+} analysis, particularly in resource limited settings. In this work, the parameters that influence the sensitivity of this approach were systematically investigated, which laid the foundation for the application of this visual amplified strategy in the detection of other analytes using DNA machines.[6] Thus, this work provides a basis for the future work aiming at the development of household devices for sensitive detection of various analytes in addition to Hg^{2+}, and our effort along this line is currently underway.

Financial support was provided by the Key Deployment Project of the Chinese Academy of Sciences (KSZD-EW-Z-021-1-4).

Notes and references

[a] *Key Laboratory of Regenerative Biology, South China Institute for Stem Cell Biology and Regenerative Medicine, Guangzhou Institutes of Biomedicine and Health, Chinese Academy of Sciences, Guangzhou 510530, China. E-mail: zeng_lingwen@gibh.ac.cn; Tel.: +86 20 32015312;*
[b] *School of Life Sciences, Anhui University, Hefei, Anhui 230601, China;*
[c] *Shenzhen Institutes of Advanced Technology, Chinese Academy of Sciences, Shenzhen 518055, China;*
[d] *Tianjin Institute of Industrial Biotechnology, Chinese Academy of Sciences, 32 XiQiDao, Tianjin Airport Economic Park, Tianjin 300308, China. E-mail: xin_xuerong@gibh.ac.cn.*
* *Joint Corresponding authors.*
‡ *Joint first authors: these two authors contribute equally to this work.*
† Electronic Supplementary Information (ESI) available. See DOI: 10.1039/b000000x/

1 T. W. Clarkson, *Ann. Rev Public Health*, 1983, **4**, 375-380.
2 F. Rouessac and A. Rouessac, *Chemical analysis: Modern instrumentation methods and techniques*. Wiley, 2007.
3 (a) K. Harano, S. Hiraoka and M. Shionoya, *J. Am. Chem. Soc.*, 2007, **129**, 5300-5301; (b) Y. Lin, C. Huang and H. Chang, *Analyst*, 2011, **136**, 863-871; L. Chen, T. Lou, C. Yu, Q. Kang and L. Chen, *Analyst*, 2011, **136**, 4770-4773; G. Wang, Z. Chen, W. Wang, B. Yan and L. Chen, *Analyst*, 2011, **136**, 174-178; L. Yan, Z. Chen, Z. Zhang, C. Qu, L. Chen and D. Shen, *Analyst*, 2013, **138**, 4280-4283; (c) K. Z. Brainina, N. Y. Stozhko and Z. V. Shalygina, *J. Anal. Chem.*, 2002, **57**, 945-949; (d) S. V. Wegner, A. Okesli, P. Chen and C. He, *J. Am. Chem. Soc.*, 2007, **129**, 3474-3475; (e) D. Li, A. Wieckowska and I. Willner, *Angew. Chem., Int. Ed.*, 2008, **47**, 3927-3931; (f) J. Yin, X. He, X. Jia, K. Wang and F. Xu, *Analyst*, 2013, **138**, 2350-2356; (g) S. Xu, L. Chen, J. Li, Y. Guan, H. Lu, *J. Hazard. Mater.*, 2012, **237-238**, 347-354.
4 Y. Tanaka, S. Oda, H. Yamaguchi, Y. Kondo, C. Kojima and A. Ono, *J. Am. Chem. Soc.*, 2007, **129**, 244-245.

Analytical Methods Accepted Manuscript

(a) C. Tang, Y. Zhao, X. He and X. Yin, *Chem. Commun.*, 2010, **46**, 9022-9024; (b) Z. Zhu, L. Xu, X. Zhou, J. Qin and C. Yang, *Chem. Commun.*, 2011, **47**, 8010-8012.
6 M. K. Beissenhirtz and I. Willner, *Org. Biomol. Chem.*, 2006, **4**, 3392-3401.
7 X. Mao, Y. Ma, A. Zhang, L. Zhang, L. Zeng and G. Liu, *Anal. Chem.*, 2009, **81**, 1660-1668.
8 G. Zhao and Y. Guan, *Acta. Biochim. Biophys. Sin.*, 2010, **42**, 722-728.
9 World Health Organization. Guidelines for drinking-water quality: incorporating 1st and 2nd addenda, Vol. 1, Recommendations, 3rd.
10 J. V. Burda, J. Sÿponer, J. Leszczynski and P.Hobza, *J. Phys. Chem. B*, 1997, **101**, 9670-9677.
11 G. T. Walker, M. C. Little, J, G. Nadeau and D. D. Shank, *Proc. Nati. Acad. Sci.*, 1992, **89**, 392-396.

Analytical Methods Accepted Manuscript

This journal is © The Royal Society of Chemistry [year]